Availability Evaluation of Micro-Grids for Resistant Power Supply During Natural Disasters

Alexis Kwasinski, *Member, IEEE*, Vaidyanathan Krishnamurthy, *Student Member, IEEE*, Junseok Song, *Student Member, IEEE*, and Ratnesh Sharma, *Member, IEEE*

***Abstract*—This paper discusses how micro-grids availability during natural disasters and in their aftermath can be assessed. The analysis focuses on two critical groups of components that allow micro-grids to improve power supply availability: distributed generators and local energy storage. For distributed generators and, due to their importance during natural disasters, this paper presents a novel focus by exploring the importance of lifelines for system availability. Renewable energy sources are identified as valuable distributed generation assets during disasters because they do not require lifelines; yet, their variable generation nature leads to the need for significant local energy storage. Additional local energy storage may be desirable as a backup solution to address potential failures that would blackout the load because they reduce the impact of lifeline performance during disasters on micro-grid availability. Analysis of micro-grids availability is performed based on Markov state space models and calculated using minimal cut sets approximations. This calculation method has the advantage of being very simple, not requiring extensive knowledge in the subject or computational needs. Results are verified with numerical experiments using Monte Carlo simulations.**

***Index Terms*—Availability model, distributed generation, energy storage, lifelines, Markov chain, microgrids, minimal cut sets, natural disasters, reliability, renewable energy sources.**

Notation

F	Set of failed micro-grid states.
W	Set of working micro-grid states.
K_j	jth minimum cut set (mcs).
$\mathrm{P}(K_j)$	mcs K_j probability of occurrence.
M_C	Total number of mcs.
c_j	Number of (failed) components in the minimum cut set j.
$u_{l,j}$	Individual unavailability of each of the c_j components in mcs K_j.
T_i	Initial time when fuel delivery may occur.
T_D	Fuel delivery due time.
T_M	Maximum amount of time a fuel delivery may occur.
u_f	Unavailability of the fuel supply system.
P_{OD}	Probability of exceeding the fuel delivery due time.
$P_{OD,\mathrm{ref}}$	Reference probability of not meeting a fuel demand reference time.
T_{TC}	Tank autonomy for the specified load.
P_E	Probability of emptying the fuel tank.
MDT_f	Mean down time of the fuel supply.
MUT_f	Mean up time of the fuel supply.
Δ	Unit energy step difference between two of the battery charge states.
P	One step transition probability matrix for the Markov chain model of the renewable source and battery system.
M	Transition rate matrix for the continuous time Markov process associated to the Markov chain represented by P.
π	Limiting distribution of the Markov chain model.
T_s	Time step length for the Markov chain.
L_{day}	Load during the day.
L_{night}	Load during the night.
P_{PV}	Power generated by the PV array at a given time.
C_{RW}	Capacity of a battery connected to a renewable source.
$\pi_{RW,W}(t)$	Probability that the renewable energy sources are in the state W at time t.
$\pi_{RW,F}(t)$	Probability that the renewable energy sources are in the state F at time t.
λ_{RW}	Failure rate of the renewable energy sources.
μ_{RW}	Repair rate of the renewable energy sources.

Manuscript received July 28, 2011; revised November 29, 2011 and March 15, 2012; accepted April 20, 2012. This work was supported in part by NEC Laboratories America, Inc. and in part by the National Science Foundation (NSF) under award # ECCS 0845828. Paper no. TSG-00275-2011.

A. Kwasinski, V. Krishnamurthy, and J. Song are with the Department of Electrical and Computer Engineering, The University of Texas at Austin, Austin, TX 78712 USA (e-mail: akwasins@mail.utexas.edu; vkrishnamurthy@mail.utexas.edu; tedsong@mail.utexas.edu).

R. Sharma is with the Department of Energy Management, NEC Laboratories America, Inc., Cupertino, CA 95014 USA. (e-mail: ratnesh@sv.nec-labs.com).

Color versions of one or more of the figures in this paper are available online at http://ieeexplore.ieee.org.

Digital Object Identifier 10.1109/TSG.2012.2197832

$f_{MG\mu}(t)$ Micro-grid's failure probability density function.

U_{MG} Micro-grid unavailability without distribution-level batteries.

$P_{MGf}(t)$ Micro-grid failure probability at time t.

μ_{FW} Sum of all the transition rates from F to W.

I. Introduction

THIS paper explores the possibility of using micro-grids as a way to improve power supply availability during natural disasters. Due to their impact on micro-grids operations during disasters and their aftermath, the analysis presents a novel approach that focuses on evaluating lifeline performance and their quantifiable impact on micro-grids availability. The presented methodology also considers the effect of added local energy storage because of their importance for reducing the effect of lifeline dependencies—a critical factor affecting micro-grids during disasters—and variability of renewable energy sources. As it is anticipated that most micro-grid owners and operators may not likely be experts in power systems or count with extensive computational capabilities, a simple availability calculation approach is presented and discussed.

A. Motivation and Problem Formulation

Recent natural disasters have created growing concerns about power supply availability and raised doubts about the capability of conventional power grids to sustain operation so vital society services—e.g., food refrigeration cycles, water provision, health care, communications, financial services, oil refining, and others—are not interrupted during disasters and in their aftermath. The experience through these disasters is that due to bulk power grids large geographical layout, combined with their centralized generation and control architectures, conventional power grids are fragile systems in which damage to less than 1% of their components can lead to extensive high-incidence outages [1] so it could be expected that large areas may experience high power grid outage probability. Thus, within the context discussed here, the grid may likely be unavailable at the critical load mains tie and its neighboring area from a few weeks to several weeks. Evidently, such performance may not be observed for all disasters or in all areas, but there is still evidence of such performance observed in various recent disasters, such as hurricanes Katrina [2] and Ike, the 2008 Sichuan earthquake in China [3], and the 2011 earthquake and tsunami in Japan (Fig. 1).

However, despite the large extension of power outages that may be observed after some natural disasters, such as hurricanes, earthquakes and tsunamis, damage assessments indicate that areas with intense infrastructure and dwellings damage is generally a much smaller area than that observed with high-incidence power grid outages. Moreover, damage distribution is very inhomogeneous and with abrupt variations in the damage severity—i.e., as Fig. 2 shows, it is very common to find a zone with extreme damage surrounded just a few meters away by areas with little damage. This characteristic is even observed in

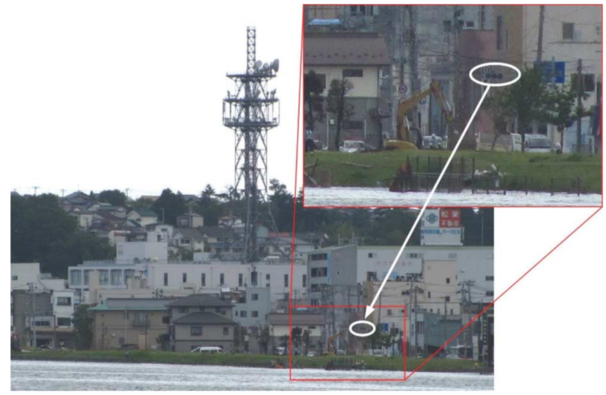

Fig. 1. Ishinomaki, Japan. The ovals highlight evidence of persisting power outages around NTT central office (the building with the large communications tower) more than 3 months after the earthquake and tsunami struck this area on March 11, 2011 (photo taken on June, 15, 2011).

Fig. 2. Onagawa, Japan. While all buildings and infrastructure in the foreground were demolished by the tsunami, there is little damage in the background area higher on the hills where the tsunami did not reach.

less extreme cases, such as after Hurricane Ike when damage to the only line serving the Bolivar Peninsula (Fig. 3) led to several weeks of lack of power in towns with extreme damage (Gilchrist), moderate damage (Port Bolivar), and little damage (High Island). From an user perspective these are two important observations that support the use of micro-grids to power electric loads during disasters because the fundamental problem for electricity consumers is the lack of powering alternatives—i.e., lack of diversity—to continuously power their loads other than conventional grids or stand-by power systems—commonly, diesel gensets. Still, these stand-by systems have also reliability issues, such as a relatively high failure to start probability for gensets that limits stand-by power plants availability to about 0.9999 or 4-nines [4].

Here, micro-grids are considered to be locally confined and independently controlled electric power grids in which a distribution architecture integrates distributed energy resources (DERs)—i.e., local distributed generators and energy storage devices—and loads [5], [6]. Hence, when micro-grids interact with a bulk grid with an interface that provides both communications and control for a coordinated operation, they could become building blocks of an advanced smart grid [7], [8]. A key fundamental difference with respect to conventional grids is that micro-grids add active network components at the distribution level, which provide more operational flexibility and reduce conventional power grids vulnerabilities caused

Fig. 3. Broken and tilted poles caused by Hurricane Ike in the only line serving the Bolivar Peninsula area.

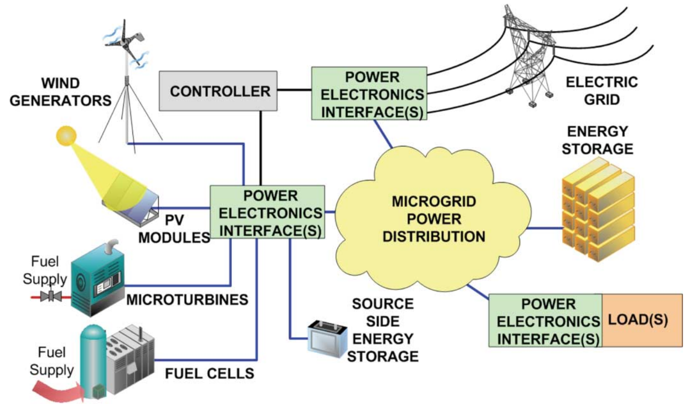

Fig. 4. General representation of a micro-grid.

by centralized generation and control architectures and long distances between power sources and loads [9]. With this approach, micro-grids contribute to locally achieve one of smart grids goals of being "*resilient to attack and natural disasters with rapid restoration capabilities*" [10]. However, potential high cost of distributed generation (DG) and local energy storage—the active network elements that are key to realize enhanced local power supply availability through micro-grids—create cost concerns that in the short term may limit application of this solution to cases in which risk assessments may include downtime cost as part of their calculations. One such risk assessment framework was presented in [11], in which the downtime cost is an important factor that contributes to make micro-grids competitive with respect to other conventional approaches. Hence, the analysis considers this more demanding case of critical loads, such as in military bases, data centers, or hospitals, where very high power availability is required because downtime costs tend to be high. Nevertheless, the analysis can also be extended to conventional loads, as indicated as part of the discussion.

One of the aforementioned observations—uneven damage distribution—provides an answer for a common concern when using micro-grids for powering a local area during disasters: micro-grid power sources can themselves be damaged, too. Yet, if the sources are located in an adequate site, chances of them being damaged are very low. Validity of this concept was recently demonstrated during the earthquake and tsunami of March 2011 in Japan, where a micro-grid in Sendai [12] was able to maintain operation powering its local loads [1]. The relevance of micro-grids in this context may be further reinforced as significant reduction of generation capacity due to safety concerns directly derived from the Fukushima #1 nuclear power plant incident leads to a long period of potential lower power quality in Japan with rotating blackouts.

Although inhomogeneous damage distribution may answer concerns about direct damage to the micro-grid, there is one potential source of problems that has been little explored: many micro-grids generation technologies, such as engine generators or microturbines, depend on other infrastructures called lifelines, such as roads or natural gas distribution networks, in order to receive fuel supply for these sources to keep them operating. These lifelines may be affected by the disasters like conventional grids are [4]. A close analysis of potential hazards at the micro-grid site may allow addressing this problem by choosing local generation sources for which their lifelines may not be severely affected by the considered hazard—e.g., natural gas supply is less vulnerable to hurricanes than to earthquakes. But, in some situations, it may not be possible to select such choice. In such situations, energy storage may be necessary in order to reduce lifeline dependencies [13]. Another option is to rely on renewable energy sources, such as solar radiation or wind that do not depend on a lifeline to reach the local micro-grid generators. However, large footprints may limit the application of these renewable energy-based power sources in sites with reduced space or relatively high power demand. Moreover, variable output also restricts the application of renewable energy sources. Like in the case of lifeline dependencies, energy storage may address this latter issue found with renewable energy sources. However, added energy storage needs due to lifeline dependencies or renewable energy sources variable output increase micro-grid capital cost with respect to the micro-grid design intended for operation during normal conditions because well designed micro-grids may not have significant requirements in terms of energy storage in order to reach high availabilities [14]. But adequate sizing of the added energy storage leads to one additional practical issue: micro-grid operators are expected to be private individuals that may not have extensive knowledge of power systems reliability theory or have extensive computational assets. Hence, quantitative assessment of lifelines and energy storage impact on micro-grids availability need to rely on a simple calculation method.

B. Previous Work and Proposed Approach

Fig. 4 shows a simplified schematic of a typical micro-grid considered for the analysis, which could have an ac, dc, or hybrid distribution system. Notice in Fig. 4 that all loads and DERs are on the micro-grid side of the power electronic interface separating the grid from the micro-grid. This interface acts as a boundary that provides electrical confinement to the micro-grid and enables implementing the availability analysis techniques used in this work. It also allows such a micro-grid to meet interconnection standards [15] and operate in an island mode enhancing local power supply availability during natural disasters when grid outages are expected to happen [16]–[19].

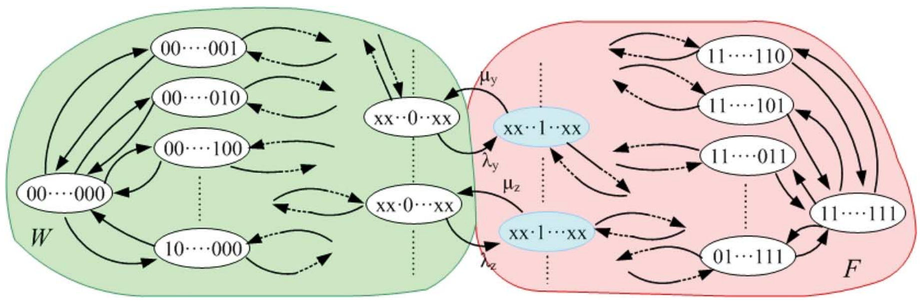

Fig. 5. General Markov representation of a micro-grid availability behavior with the minimal cut states indicated with a shaded interior.

During natural disasters, micro-grids are expected to operate in island mode. Hence, power supply availability is predominately influenced by micro-grids DERs performance [20]–[22]. Hence, the discussion is oriented towards DER and, in particular, effect on availability from local energy storage and lifelines. Thanks to micro-grids confined electric domain, their availability can be studied with somewhat simpler approaches that those used to assess conventional power distribution reliability [23]. One example of such alternative approaches using minimal cut sets (mcs) theory. An mcs can be related to a group of failed components such that when all of those components are in a failed state, the system is also in a failed state—characterized here by the impossibility of completely feeding the load—but if any single one of those components is repaired, then the system is back again into an operational state. Such approach can be found in [22] and [24] but their focus is not on lifelines or energy storage as we present here. A relevant result in [24] is to identify the importance of having diverse power sources—while redundancy refers to having more of the same components than the minimum required, diversity implies having different entities serving the same goal. In the past there has also been a number of works studying micro-grids availability including [25]–[36]. Yet, although lifeline performance—e.g., roads to deliver fuel—is a critical aspect of micro-grid availability the only basic diesel fuel delivery availability model have only been recently suggested in [13] and only for stand-by operation and not for continuous operation as needed in micro-grids. Instead, past analyses have been oriented to other micro-grid portions, such as power distribution [31], or renewable sources energy profile characterization in an average sense [36], or local DG units [31]–[33] (still, without considering their fuel supply) That is, past work explores DG generators reliability performance without considering that, in turn, these sources cannot operate if they are not fueled, and that such fuel supply is dependent on lifeline performance.

In this paper, Section II presents a simple approach to calculate micro-grids availability using mcs with special focus on modeling lifelines performance and the effect of energy storage—both aspects not previously explored in the literature—because of their importance for micro-grid performance during disasters. Case studies are presented in Section III and calculations performed with the presented mcs approach are compared with Monte Carlo simulations used as an experimental validation mean. Finally, this paper concludes with a summary of its main findings in Section IV.

II. Micro-Grid Availability Calculation Methodology

A. System Availability Calculation Approach

Consider the general Markov representation in Fig. 5 for a micro-grid like the one in Fig. 4. In Fig. 5, each state is represented by a binary number in which each digit represents the operating state of a micro-grid component. A "1" indicates a failed state and a "0" indicates an operating state. Although this model may initially seem complicated because even for micro-grids there are a large number of states, an mcs approach allows to greatly simplifying the analysis. For system components that are reliable enough, each mcs can be associated with a shadowed state in Fig. 5—called minimal cut state [37]—at the boundary between the set F of failed micro-grid states and the set W of working micro-grid states. The micro-grid unavailability U_{MG} can be calculated with [37]

$$U_{MG} = \mathrm{P}\left(\bigcup_{j=1}^{M_C} K_j\right) \cong \sum_{j=1}^{M_C} \mathrm{P}(K_j) = \sum_{j=1}^{M_C} \prod_{l=1}^{c_j} u_{l,j} \quad (1)$$

where K_j represents the mcs, $\mathrm{P}(K_j)$ is the mcs probability, M_C is the total number of mcs, c_j is the number of (failed) components in the mcs K_j, and $u_{l,j}$ is the individual unavailability of each of the c_j components in mcs K_j. In the analysis, $u_{l,j}$ is the ratio of the component failure rate $\lambda_{l,j}$ to the sum of its failure rate $\lambda_{l,j}$ and repair rate $\mu_{l,j}$. Failure and repair rates are practically calculated by taking the inverse of the mean up time (MUT) and mean down time (MDT), respectively. The error in the approximation in (1) can be evaluated considering that [37]

$$\sum_{i=1}^{M_C} \mathrm{P}(K_i) - \sum_{i=2}^{M_C} \sum_{j=1}^{i-1} \mathrm{P}\left(K_i \bigcap K_j\right) \leq U_{MG} \leq \sum_{i=1}^{M_C} \mathrm{P}(K_i). \quad (2)$$

Although an mcs approach is simpler than Markov-based methods, in some systems it may be tedious to identify all the mcs. This task can be simplified and automated by recognizing that given systems structures (from an availability perspective) give rise to specific mcs. Consider the following most common availability relationship of system's elements under the assumption of reliable components [the error bound implied in this assumption can be assessed by (2)]:

a) Series configuration: Consider Fig. 6 where all components in the micro-grid need to be operational in order to power the load. This configuration, then, constitutes from an availability perspective a series connected group of components—in an electrical circuit, this functional reliability relationship in series may or may not correspond to their electric topological layout; e.g., essential electrical components that in a circuit are connected in parallel may be represented as a series connection from an availability perspective. Thus, each mcs is associated with the failure of a given system component while all other components are considered to be operational. Hence, the probability of each mcs of occurring equals the unavailability of the failed component associated with such mcs, so the system unavailability under the assumption of reliable components is approximately equal to the sum of their unavailabilities. The transition rate from the minimal cut states into W is the sum of the repair rates of the components in the series configuration.

b) Parallel configuration: Consider Fig. 7 with a parallel combination of two paths, each path with a series combination of components. For the micro-grid to power the load it is necessary that all components in at least one of the two paths are operational. Each mcs is, then, formed by one component from each path—e.g., one mcs in Fig. 7 is formed by the natural gas supply in the top path and the DG unit #2 in the bottom path—so the number of mcs yielded by this configuration equals the product of the number of components in one path by the number of components in the other path. The probability of each mcs is the product of unavailabilities of each of the components in the mcs. That is, the probability of each mcs equals the product of unavailabilities of a component in each path. This general description of a parallel configuration of two paths can be directly reduced to a simple parallel configuration by considering only one component in each path, which results in only one mcs with probability equal to the product of unavailabilities of all the components in the parallel configuration. The sum of the transition rates from all minimal cut states to W equals the sum of the repair rate of each component multiplied by the number of components in the other parallel path.

c) $n + 1$ redundant configuration: In this case, a total of ${}_{n+1}C_2$ mcs are formed representing all possible groupings of two of the $n + 1$ components in the redundant arrangement. Since it is assumed that all components in the redundant arrangement are equal, the probability of each mcs is the square of the unavailability of each component. The number ${}_{n+1}C_2$ equals [38]

$${}_{n+1}C_2 = \frac{n+1!}{2!(n-1)!}. \quad (3)$$

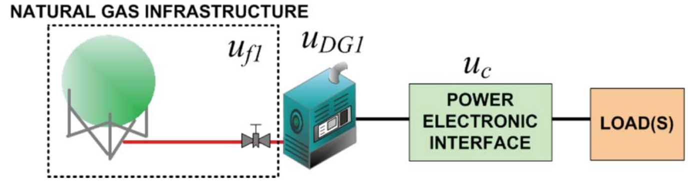

Fig. 6. Scheme for a micro-grid with one power supply path to the load.

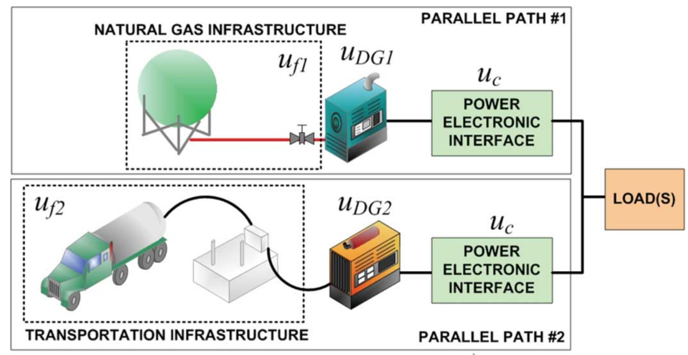

Fig. 7. Scheme of a micro-grid in which the load can be powered from two power paths.

These three general cases typically represent the most common arrangements that can be found in practical micro-grids. Hence, a combination of them can yield all necessary mcs of a micro-grid without significant complexities. From [24], it is also possible to identify failure and repair rates for each type of configuration. Once mcs are identified, the next step is to calculate the unavailability of each component. For most components, such as power electronic interfaces, distribution cables and local DG sources, there exists industry information with failure rates, such as [39]. As it was explained above regarding inhomogeneous damage distribution during disasters, if the micro-grid is located in a site where observed damage is not extreme, then these values for these particular micro-grid components should not change during disasters. Repair rates can be evaluated for these components based on known or assumed maintenance, logistical and repair processes. However, these common approaches may not be applied to renewable sources because of their variable stochastic nature. Neither can these common approaches be used to sources that has a discontinuous fuel delivery model—e.g., diesel carried to the micro-grid site through trucks—or to added energy storage. The discussion that follows next aims at addressing these other challenges.

B. General Analysis Assumptions

In addition to particular assumptions considered in the analysis and discussed at the point where they are relevant, the proposed methodology considers some general assumptions worth emphasizing here. As mentioned, one of the general assumptions is that, based on damage assessment experiences (e.g., Figs. 1–3) and collected extensive outage data, the conventional power grid around the micro-grid may likely fail for several weeks as a result of a natural disaster even when the damage in such area is light. The micro-grid is assumed to be located in one of such areas with light damage but extensive power outages. The use of the term availability is chosen in this work in order to emphasize the fact that the studied entities can be repaired when they fail so it is possible to distinguish its use from the term reliability which applies to non-repairable components [37]. Hence, in such use of the term availability, it is being relaxed the implicit assumption that availability—or more strictly steady-state or asymptotic availability—may only apply to processes in a long-run sense, and it is used, instead, in a more general sense as it may be associated to the use of availability for repairable components or entities that operate in standby regimes [37]. Another general assumption is that, for simplicity and in order to relate the discussion with the typical load profile found in a critical load represented by a digital communications facility, such as that in Fig. 1, the load is assumed to be constant and known. Such load can also be associated with the expected (average) value of a variable load. However, this assumption is not a requirement for the proposed model that can also consider instantaneously uncertain loads. Yet another general assumption considered in the analysis is that, since stability study is out of the scope of this work, the micro-grid under evaluation has already been designed and engineered ensuring adequate stability. Finally, lifelines failure and repair rates are considered to take typical values found during disaster conditions or in their aftermath. These values vary depending the intensity of the disaster.

C. Model for Continuous Delivery of Fuel Supply

In most micro-grid applications, this model applies to natural gas for microturbines, internal combustion engines, or fuel cells with local reformers. Hence, a natural gas distribution system is the lifeline for these sources. Information about MUT and MDT for natural gas supply can be obtained from their suppliers or from studies [40] and be adjusted to natural disasters conditions without difficulty.

D. Model for Discontinuous Delivery of Fuel Supply

Let us consider the case of a local source, such as a diesel generator, that requires periodic delivery of fuel which is stored on-site in a tank. For simplicity consider that the micro-grid load is known and constant so the tank capacity provides a known autonomy of T_{TC}. Such load may be, typically represented, by a modern digital communications center, already identified as a critical site during disasters [41]. For variables loads with a given uncertainty, the expected (average) value of such load can be considered for the calculations because for operation in an aftermath of a natural disaster, load changes occur at a time scale much shorter—e.g., in the order of minutes—than the necessary local energy storage, in this case represented by T_{TC}—in the order of hours or days. In this case, the roads network is the lifeline for the micro-grid so the time, t_d, at which the fuel is delivered to the micro-grid site is a random variable that depends on a fuel delivery probability density distribution function $f_d\ (t_d)$. Although $f_d\ (t_d)$ can take many forms, some of those, like an exponential distribution applied in [24], are not realistic. Some of the issues found with the exponential distribution includes the fact that its maximum is found at its initial time T_i instead at the defined delivery time T_D, and then it decreases continuously within a semi-infinite time interval $[T_i, \infty)$—i.e., there are non-zero chances of receiving the fuel delivery in a time instant infinitely away in the future. Instead, a triangular form proposed here is a realistic representation that at the same time does not cause excessive calculations complexities. In order to represent a realistic fuel delivery process, it is assumed that there is a fuel contract that establishes a due delivery time indicated by T_D, when it is more likely to have the fuel delivered. Fuel can be delivered from some initial time T_i and it is certain that fuel cannot be delivered before T_i. Then, the probability of having the fuel delivered increases linearly until T_D when it reaches its maximum. Still, fuel delivery may be overdue and occur until a maximum possible time T_M. After T_M passes, fuel delivery can no longer occur or is no longer accepted. For simplicity, the decreasing fuel delivery probability between T_D and T_M is assumed to decrease linearly. This triangular distribution is, then

$$f_d(t_d) = \begin{cases} 0, & 0 \le t_d < T_i \\ \frac{2(t_d - T_i)}{(T_M - T_i)(T_D - T_i)}, & T_i \le t_d \le T_D \\ \frac{-2(t_d - T_M)}{(T_M - T_i)(T_M - T_D)}, & T_D \le t_d \le T_M. \end{cases} \quad (4)$$

In order to represent the overdue delivery process T_M is considered to be given by

$$T_M = \frac{T_D - T_i P_{OD}}{1 - P_{OD}} \quad (5)$$

where P_{OD} is the probability of exceeding the fuel delivery due time. That is, P_{OD} represents the chances of having an overdue fuel delivery so the difference between T_D and T_M accounts for a potential delay—i.e., loss of performance—of the transportation infrastructure. There are several studies in the literature and, in particular, in logistics and transportation sciences dedicated to evaluate P_{OD} [42]–[46]. In normal conditions, P_{OD} may take values at most in the single digit percentage points or lower. However, during disasters, data from typical transportation delays observed after disasters make P_{OD} to take values from 0.2 to 0.6 and higher, depending on the disaster intensity. A simple and reasonable approach from [13] considers that P_{OD} varies linearly from being 1 when the time interval ΔT_D between T_D and T_i—i.e., ΔT_D is T_D–T_i—is 0 to being 0 when ΔT_D equals a time interval, $\Delta T_{D,0}$, that is long enough to ensure that fuel delivery will be for sure delivered on time—i.e., $P_{OD} = 0$ when $\Delta T_D = \Delta T_{D,0}$. Hence

$$P_{OD} = 1 - \frac{\Delta T_D}{\Delta T_{D,0}} \quad \text{for } 0 \le \Delta T_D \le \Delta T_{D,0} \quad (6)$$

and

$$\Delta T_{D,0} = \frac{\Delta T_{D,\mathrm{ref}}}{1 - P_{OD,\mathrm{ref}}} \quad (7)$$

where $P_{OD,\mathrm{ref}}$ is the probability of exceeding T_D corresponding to a known interval $\Delta T_{D,\mathrm{ref}}$. For example, consider that $T_D =$ 72 h, $T_i = 48$ h, and that $P_{OD} = 0.3$ when $\Delta T_D = 24$ h. Then, $T_M = 82.28$ h so $\Delta T_{D,0} = 82.28 - 72 + 24 = 34.28$.

Now, assume for simplicity that the inter-arrival time between each truck can be assumed to be independent and identically distributed. It is also assumed that the truck instantaneously replenishes the fuel tank and leaves and the next truck arrives at the location after a random time with identical probability density function than the previous truck. Since refueling occurs instantaneously, the generator's engine fuel supply from the diesel tank at the engine's fuel intake will essentially determine the unavailability of the fuel supply system. That is, when the diesel tank is empty the fuel supply system is at a failed state. Since it is assumed that the load is constant and known (or for a variable load represented by its expected value over T_{TC}), the tank autonomy T_{TC} provides an indication of the probability of emptying the fuel tank P_E when the fuel delivery time exceeds T_{TC}

$$P_E = P\{t_d > T_{TC}\} = 1 - P_{E^*} = 1 - \int_{t_d=0}^{t_d=T_{TC}} f_d(t_d)\, dt_d. \tag{8}$$

Evidently, choosing T_{TC} long enough so it exceeds T_M would ensure that $P_E = 0$, but the problem at hand here is that when the micro-grid is planned, T_{TC} may likely be estimated for normal operating conditions when both P_{OD} and T_M are much lower values than what it can be obtained when they are calculated based on natural disaster conditions. Hence, T_{TC} calculated under normal conditions may likely be less than T_M calculated during natural disasters conditions, as it is evaluated in this work.

In order to find the fuel supply unavailability indicated by this process, consider that based on the relaxed assumption about the definition of availability in Section II-B that a very large number of refueling cycles have passed because the grid power outage lasts at least a few times longer than T_{TC}. It can be expected that in $100P_E$ percent of these cycles the fuel delivery truck arrived after T_{TC} with an expected fuel supply down time of MDT_f. Conversely, it can be expected that in $100P_{E^*}$ percent of the cycles the fuel truck arrived before T_{TC} so the generator did not fail due to fuel starvation. It can be noted that there are $r = P_{E^*}/P_E$ fuel delivery cycles in which the truck arrived before T_{TC} for every fuel delivery cycle in which the generator stops operating after running for T_{TC} hours because the tank was emptied. Hence, in an average sense and over a very large number of cycles it can be expected that r refueling cycles lasting in average T_{E^*} are immediately followed by one refueling cycle in which the generator fails during a time T_E after running for T_{TC} hours because it is out of fuel. That is, according to this described process and assuming that T_{TC} is selected within the interval $[T_D, T_M]$, the MDT_f for a generator fuel supply model equals

$$\mathrm{MDT}_f = T_E = \frac{T_M - T_{TC}}{3} \tag{9}$$

whereas the MUT_f is

$$\mathrm{MUT}_f = rT_{E^*} + T_{TC} \tag{10}$$

where for $f_d(t_d)$ given by (4) T_{E^*} is shown in (11) at the bottom of the page. The choice for T_{TC} selected within the interval $[T_D, T_M]$ considers that for the aforementioned reasons—that T_{TC} is estimated for normal conditions whereas T_M is now calculated during extreme events—the option $T_{TC} > T_M$ may be an unrealistic and trivial scenario, and that a micro-grid planer would rarely choose a tank autonomy shorter than the fuel delivery due time.

Based on this analysis the unavailability of the fuel supply system is, then

$$u_f = \frac{\mathrm{MDT}_f}{\mathrm{MUT}_f + \mathrm{MDT}_f} \tag{12}$$

with failure and repair rates, λ_f and μ_f equal to the inverse of MUT_f and MDT_f, respectively. For example, in the case of $T_D = T_{TC} = 72$ h, $T_i = 48$ h, $T_M = 82.28$ h, MUT_f equals 221.3 h, MDT_f equals 3.4 h, and the fuel supply availability $a_f = 1 - u_f$ is 0.985.

E. Model for Renewable Energy Sources

As it was mentioned, renewable energy sources may be suitable to sustain micro-grid operation during natural disasters because they do not require lifelines. However, their variable output nature complicates their application. In order to address their variable output nature—part stochastic and part deterministic—of renewable energy sources, it is assumed here that energy storage is added on the renewable energy-based distributed generators side of the micro-grid. With this added energy storage these variable renewable energy sources can be considered to be more dispatchable and have a given availability determined by the capacity of the added energy storage and the solar or wind energy profiles. Thus, a Markov chain model indicated in Fig. 8 is used to model energy states in the energy storage system associated to a given renewable energy source. As shown in Fig. 8, each state represents an energy level for the storage system, so each state transition, characterized by a probability p_i or p_{-i}, represents a charge or discharge process. For example, State #1 symbolizes the energy level of storage when it is fully discharged, and State #*N* symbolizes the energy

$$T_{E^*} = \frac{(T_M - T_D)\int_{T_i}^{T_D} t(t - T_i)\, dt + (T_D - T_i)\int_{T_D}^{T_{TC}} t(T_M - t)\, dt}{(T_M - T_D)\int_{T_i}^{T_D} (t - T_i)\, dt + (T_D - T_i)\int_{T_D}^{T_{TC}} (T_M - t)\, dt} \tag{11}$$

This article has been accepted for inclusion in a future issue of this journal. Content is final as presented, with the exception of pagination.

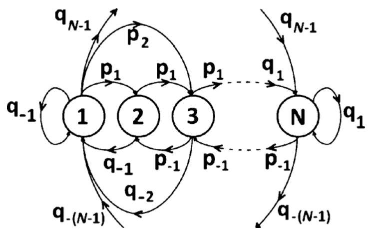

Fig. 8. Markov chain diagram.

level when it is fully charged. If it is assumed that the energy storage devices have linear charge and discharge processes, the energy difference between any two adjacent states is Δ so the power involved in such process is Δ divided by the time step T_s between two consecutive steps in the Markov chain. Hence, p_{-i} generally represents the probability of a transition among states with an energy efflux of $i\Delta$ in T_s, and p_i represents the probability of a transition among states with an energy influx of $i\Delta$ in T_s, with i taking values from 1 to $N-1$. Then, the one-step transition probability matrix, P, is

$$P = \begin{bmatrix} q_{-1} & p_1 & p_2 & p_3 & \cdots & & & \\ q_{-1} & 0 & p_1 & p_2 & \cdots & & & \\ q_{-2} & p_{-1} & 0 & p_1 & \cdots & & & \\ q_{-3} & p_{-2} & p_{-1} & 0 & \cdots & & & \\ \vdots & \vdots & \vdots & \vdots & \ddots & & & \\ & & & & & 0 & p_1 & q_2 \\ & & & & & p_{-1} & 0 & q_1 \\ & & & & & p_{-2} & p_{-1} & q_1 \end{bmatrix}_{N\times N} \tag{13}$$

where

$$q_{-1} = 1 - \sum_{i\in S} p_i \tag{14}$$

$$q_1 = 1 - \sum_{i\in S} p_{-i} \tag{15}$$

$$q_{-k} = 1 - \left(\sum_{i=1}^{k-1} p_{-i} + \sum_{i\in S} p_i \right) \tag{16}$$

$$q_k = 1 - \left(\sum_{i=1}^{k-1} p_i + \sum_{i\in S} p_{-i} \right). \tag{17}$$

The transition probabilities terms indicated by the terms q_k correspond to the particular cases when there is an overflow or a demand of energy greater beyond the battery capacity range. Like for the other terms, a negative subscript corresponds to a battery discharge process and a positive subscript indicates a battery charge process.

Consider first the case in which the renewable energy sources are made of a PV array. Since each state in Fig. 8 represent the energy level of the energy storage devices—e.g., batteries—transition among states will depend on the power difference between generated and consumed power at the micro-grid. For simplicity, the load is assumed to be constant and known or to be represented by the expected (average) value of a variable load. However, this assumption is not a requirement for the proposed model that can also consider instantaneously uncertain loads. In order to obtain the values for the probabilities p_i and p_{-i} of each Markov chain transition, it is first necessary to realize that the power balance P_B is

$$P_B = (P_{PV} - L_{\text{day}} - L_{\text{night}}) = P_{PV} - 2L \tag{18}$$

where L is the load, which is considered for simplicity of the discussion the same both during the day, L_{day}, and night, L_{night} (different values for L_{day} and L_{night} could also have been considered as part of the calculations) and P_{PV} is the power generated by the PV array. Then, a histogram of actual PV generated power at the micro-grid site during a 12-h period is used to characterize PV generation at the site through a probability density function. This distribution is used as an input for a Monte Carlo process in order to generate random PV generated power P_{PV} at each Markov chain time step. The application of a Monte Carlo approach provides the necessary uniform discretization process for the generated PV power. Since the load is known and the PV generated power is now known, the power balance for each Monte Carlo run and the number of occurrences for each power balance value are also known, which, in turn, is used in order to estimate the state transition probabilities p_i and p_{-i}. Since the PV generated power histogram considers data for a 12-h period when the load is $L_{\text{day}} = L$, the power balance (18) adds an equal load L in order to consider that the output of the PV array and energy storage needs to sustain the load during the entire 24-h period, which implies that the night load is effectively shifted to daytime as a battery charging load for the PV array.

Once the one-step transition probability matrix, P, is known, the limiting probabilities vector, π, can be found from [47]

$$\pi = \pi\, P \tag{19}$$

where each of the components in π represents the long term steady state probabilities that the energy storage system is at a certain energy state—e.g., π_1 represents the probability that energy storage is at State #1. Finally, system unavailability u_{RW} can be calculated considering that the load is not fully powered when energy storage is at state i and the load requires an energy of $i\Delta$ or more for one time step T_s of the Markov chain. Considering all possible transitions from all possible states for the considered time step, the unavailability is

$$u_{RW} = \sum_{i\in\{1,N-1\}} \left(p_{-i} \sum_{j\le i} \pi_j \right). \tag{20}$$

Energy storage capacity, C_{RW}, affects unavailability by realizing that

$$C_{RW} = (N-1)\Delta \tag{21}$$

so C_{RW} can be changed by modifying Δ, which, in turn, changes P and, hence, u_{RW}.

This same analysis can be extended to the case of a hybrid micro-grid with PV and wind energy power generators so their diverse source of energy could reduce the required energy storage capacity. In this case, if it is assumed that each of the renewable sources could power the load alone when their source of energy is present, then the power balance equation is

$$P_B = (P_{PV} + P_W - L_{\text{day}}) + (P_W - L_{\text{night}}) \\ = P_{PV} + 2(P_W - L). \quad (22)$$

As an example, consider a micro-grid with a 100-kW load. In order to provide some generation overhead consider that only a PV array of 1.225 MW is used—which gives an average power generation of 293.63 kW $(\text{variance} = 68.2)$ during daytime, i.e., 7:00 am to 7:00 pm. By following the described approach, the PV curve in Fig. 9 can be found. Suppose that the load is a critical one—e.g., a communications site—so a 5-nine availability is sought for the sources. Then, Fig. 9 indicates that 1.15-day capacity of energy storage is needed which translates into a battery capacity of 2.7 MWh obtained for a time step T_S of 1 h, and with Δ/T_S and N equal to 10 kW and 277, respectively. When 225 kW of wind power generators are added, yielding 110.82 kW of average generated wind power—so each wind or PV generators can sustain the load alone—the necessary energy storage to achieve an availability of 5-nines decreases significantly. Both solar and wind data for this example were obtained from actual measurements performed in Austin during the same time periods, and, hence, they naturally and implicitly consider profile correlation existing between these two renewable energy sources. As Fig. 9 represents, with this diverse pool of sources energy storage requirements dropped to about 0.5 days worth of load power, or 1.2 MWh. If only a 2-nine target availability is sought, 960 kWh—equivalent to 0.4 days—of energy storage are needed when only the PV array is considered, and 720 kWh—equivalent to 0.3 days—are needed for the combined PV and wind case.

The failure and repair rates for these sources can be obtained by considering that the Markov chain in Fig. 8 is the embedded Markov chain for a 2-state Markov process in which a state S_0 represents the renewable energy power source failure condition—inability to power the load fully which corresponds to the condition described by (20)—and the other state S_1 represent the opposite situation. The equivalent Markov process is described, then by

$$\dot{\pi}^T_{RW}(t) = \pi^T_{RW}(t)M \\ = (\pi_{RW,W}(t) \quad \pi_{RW,F}(t)) \begin{pmatrix} -\lambda_{RW} & \lambda_{RW} \\ \mu_{RW} & -\mu_{RW} \end{pmatrix} \quad (23)$$

where the superscript index "T" represents a transpose operation, $\pi_{RW,W}(t)$ is the probability of having the system operating in state S_1 at time t, $\pi_{RW,F}(t)$ is the same probability for S_0, M is the transition rate matrix for the 2-state equivalent Markov process with failure rate λ_{RW} and repair rate μ_{RW}. The Markov chain and Markov process are related by [47]

$$M = \gamma(P - I) \quad (24)$$

where I is the identity matrix and γ is obtained from [47]

$$\gamma = \frac{1}{T_S}\frac{p_{11}}{1 - p_{11}} \quad (25)$$

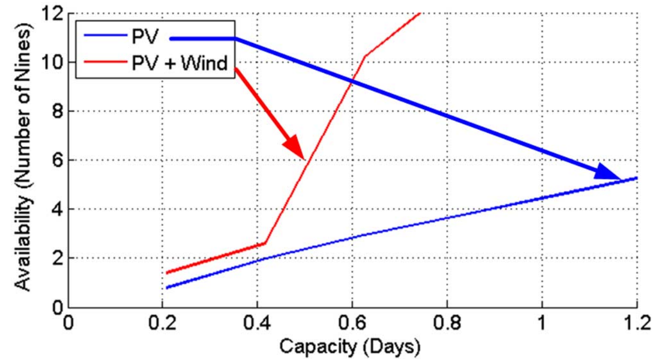

Fig. 9. Availability versus energy storage capacity.

where p_{11} is the term in row #1 and column #1 of P, i.e., it equals q_{-1}. Hence, for the 100-kW load powered by PV and energy storage combination and a target availability of 5-nines, $\lambda_{RW} = 5.252\ 10^{-6}$ and $\mu_{RW} = 0.5252$, whereas for the case with added wind generators $\lambda_{RW} = 8.189\ 10^{-6}$ and $\mu_{RW} = 0.8189$. When the target availability is 2-nines, $\lambda_{RW} = 5.2\ 10^{-3}$ and $\mu_{RW} = 0.512$ when only the PV array is present, $\lambda_{RW} = 7.3\ 10^{-3}$ and $\mu_{RW} = 0.7219$ when PV is combined with wind energy.

F. Model for Power Distribution Level Energy Storage

In addition to source-level energy storage—e.g., in stored diesel for an internal combustion engine generator or in batteries for a PV system—it may be desired to add additional energy storage at the micro-grid distribution level—e.g., at the main bus—in order to further increase availability. For example, in the recent earthquake that affected Japan, local energy storage was a key aspect of keeping the micro-grid in Sendai [1] operating. Consider now Fig. 5. From [37] and [48], the probability density function $f_{MG\mu}(t)$ associated with the probability of leaving the set F at time $t + dt$ after being in F from $t = 0$ is

$$f_{MG\mu}(t) = \mu_{FW} e^{-\mu_{FW} t} \quad (26)$$

where μ_{FW} is the sum of all the transition rates from F to W. Since each of the minimal cut states at the boundary between F and W can be associated to an mcs, μ_{FW} can be calculated once the mcs are known. Then, the probability of discharging the batteries while the system is in F since $t = 0$ is the probability of leaving F at a time longer than the battery backup time T_{BAT}. Hence

$$P_{BD} = P\{t > T_{BAT}\} = 1 - \int_{\tau=0}^{\tau=T_{BAT}} f_{MG\mu}(\tau)d\tau \\ = e^{-\mu_{FW} T_{BAT}}. \quad (27)$$

The micro-grid failure probability $P_{MGf}(t)$ is, then, the probability that the system failed at $t = 0$ and the batteries discharged. If it is assumed that the micro-grid had been turned into operation a very long time in the past, then $P_{MGf}(t)$ equals the unavailability of the micro-grid U_{MG} without distribution-level batteries, which is obtained from (1). Thus, the micro-grid unavailability with added batteries at the distribution level is

$$U_{MG,T} = U_{MG} e^{-\mu_{FW} T_{BAT}}. \quad (28)$$

III. Case Studies

Several case studies were considered in order to evaluate the previous discussion. These cases are:

- Case 1: Load fed through converters by a microturbine fueled by natural gas (represented in Fig. 6).
- Case 2: Same as Case 1 but with two microturbines in parallel so each of them can power the load alone.
- Case 3: Load fed through converters by an engine generator fueled by diesel delivered by truck and stored in a local tank.
- Case 4: Same as Case 3 but with two engine generators in parallel so each of them can power the load alone.
- Case 5: Two power paths to the load; one is as indicated by Case 1 and the other by Case 3. Each path can power the load alone (represented in Fig. 7).
- Case 6: Combined PV and energy storage powering the load through a converter.
- Case 7: Same as Case 6 but combining PV and wind.
- Case 8: Same as Case 5 but with the diesel generator path replaced by the path indicated in Case 6.
- Case 9: Same as Case 5 but with the diesel generator path replaced by the path indicated in Case 7.

These cases assume that the potential hazard at the micro-grid site is a hurricane so natural gas supply availability is still high [4]. However, transportation infrastructure has a poor performance so the value for P_{OD} is relatively high, indicating high chances of delays. Component parameters are shown in Table I—unless clarified otherwise those are the same values used throughout this paper—and results of the calculations in Table II. Two options are considered for the renewable energy sources in cases 6 to 9: subcase "a" considers that there is sufficient energy storage to yield an availability of 5-nines at the output of the renewable energy source and sub-case "b" considers that their output availability is 2-nines. Parameter values for the PV or PV + wind combined with energy storage are those discussed in Section II-E. In a practical setting, the outcome of the analysis of power output availability for renewable sources combined with energy storage could be presented in tables or simple to read graphs, such as that in Fig. 9. All converters are assumed to be in an $n+1$ redundant configuration with $n=6$. Comparison between unavailabilities calculated with mcs and with Monte Carlo yield almost identical results. However, the mcs approach is extremely simple to calculate. In these particular examples presented here, calculations involving mcs did not require the use of computers and only a simple calculator was used. Such simplicity leads to two benefits: for the expert operator of a micro-grid, simple calculations reduce the chances of involuntary calculation mistakes, but for the more common case of a micro-grid operator that is not an expert in power systems—e.g., an infrastructure manager in a hospital or a data center manager—the proposed approach provides a way to assess micro-grid availability in order, for example, to perform quantifiable risk assessments. Still, one potential weakness of the proposed method is that it may lead to some errors because, as (1) indicates, the calculation involves approximations. Nevertheless, the proposed method allows quantifying the boundary of such error with (2). For example, consider here Case 3 which is the one more prone to error due to the relatively low availability of the diesel delivery process. The exact unavailability of this case based on the availability of the three components in the series arrangement—the diesel supply, the diesel generator, and the converters—is 0.02101 whereas the unavailability obtained by the mcs approach obtained by summing the unavailabilities of the diesel supply, the diesel generator, and the converters is 0.021103. The error, as indicated by the second term of the left side of the inequality in (2), is calculated by summing the three terms that represent the product of the unavailabilities of two of the three components (components in the series arrangement) considered in this case. Such calculation yields that the error is $9.156\ 10^{-5}$. When this error is subtracted from the mcs obtained unavailability of 0.021103, the result is 0.02101 which coincides with the exact unavailability value.

Another important advantage of the proposed approach is that it provides valuable planning insights about the micro-grid. High diesel fuel supply unavailability yields no significant availability improvement when paralleling generators (cases 3 versus 4) because diesel fuel supply is the determining component for availability calculation. However, such improvement is evident with microturbines (cases 1 versus 2) because the limiting component is the microturbine. Yet, in order to reach 6-nines availability the cases with microturbine require significant more energy storage than those with diesel generators. This observation seems to be counterintuitive based on the base unavailability of these cases. The explanation is found when the MDT for the micro-grid in each case is calculated. While

TABLE I
Reliability Values Used in the Case Studies

Item and origin of the value	μ (1/hours)	Unavailability u
Diesel generator [24]	0.2	0.0061
Microturbine [24]	0.02	0.006
Natural gas supply [24]	0.02	$2.5\ 10^{-5}$
Diesel fuel supply [current paper]	0.294	0.015
Converter [24]	0.003	$3.33\ 10^{-4}$
$n+1$ arrangement of 7 converters	0.012	$3\ 10^{-6}$

TABLE II
Case Studies Evaluation Results

Case #	U_{MG} (mcs-based)	U_{MG} (Monte Carlo-based)	μ_{FW}	T_{BAT} for $U_{MG,T}$=1 10^{-6}
1	0.006028	0.0060836	0.052	167.4 hrs
2	0.000064	0.000068	0.072	57.76 hrs
3	0.0211	0.02103	0.506	19.67 hrs
4	0.01504	0.014986	0.706	13.62 hrs
5	0.000127	0.000124	1.674	2.89 hrs
6.a	0.000013	0.0000146	0.538	4.28 hrs
6.b	0.010003	0.0100265	0.524	17.57 hrs
7.a	0.000013	0.0000141	0.8309	3.09 hrs
7.b	0.010003	0.0100051	1.5408	5.97 hrs
8.a	$0.78\ 10^{-7}$	0.0000001	1.718	N/A
8.b	0.0000603	0.0000598	1.676	2.44 hrs
9.a	$0.78\ 10^{-7}$	0.0000002	2.6	N/A
9.b	0.0000603	0.0000597	2.3	1.78 hrs

the micro-grid in Case 1 has an MDT of 48.3 h (repair rate of micro-grid $\mu_{MG} = 0.0207$), the micro-grid in Case 3 has an MDT of 4.29 ($\mu_{MG} = 0.233$) because diesel generators tend to be simpler to repair than microturbines. That is, a micro-grid with microturbines need more stored energy because although it is more unlikely to fail, when it fails—and that is when the added energy storage is needed—it is likely to stay in the failed state longer. Although renewable energy sources do not have lifelines, they require significant energy storage in order to reach desired levels of availability. This issue combined with their large required footprint limits their application. In all cases, diverse power sources contribute to improve availability and reduce the need for local energy storage. Hence, Case 5 seems to be the most suitable choice in this case. Moreover it is the most cost effective of all. Another potential alternative to Case 5 is Case 2 with the microturbines replaced by natural gas internal combustion engines. However, this last option may be unsuitable in case of earthquakes when the unavailability of natural gas supply is worse than with hurricanes. Still, if precautions are taken so adequate availability for natural gas is ensured, this last option is also adequate for earthquakes, as practically demonstrated by the aforementioned micro-grid in Sendai, whose power sources were 2 natural gas generators and at least 20 minutes worth of batteries.

IV. Conclusion

This paper evaluates micro-grids availability oriented towards operation during natural disasters and their aftermath. A key contribution of this paper is to focus on representing the effect of two critical aspects affecting micro-grid availability during natural disasters and in their aftermath: lifelines performance and local energy storage contribution. Such representation is done by presenting and discussing their availability models. The selected calculated approach is based on minimal cut sets theory. It is shown that this approach involves extremely simple calculations that do not require computers or extensive theoretical knowledge on the matter in order to assess micro-grid availability. Moreover, if desired, the proposed approach allows quantifying the error involved in the availability calculations.

Theoretical calculations confirmed with Monte Carlo simulations seem to show that in the context of natural disasters micro-grids may achieve availabilities much higher than conventional grids, making micro-grids a prime option for developing advanced smart grids. Still, local energy storage and diverse energy sources are required in order to achieve high availabilities. Although renewable energy sources have been identified as a suitable choice to power micro-grid during natural disasters because they do not require lifelines, large footprints, high cost, and the need for significant added energy storage limit their application.

Future research will involve studying alternative fuel delivery probability distribution functions and modeling the availability of both fixed and portable standby diesel generators.

Acknowledgment

The authors would like to thank Dr. W. Grady at The University of Texas at Austin for providing the solar and wind data.

References

[1] B. Fahimi *et al.*, “Charge it,” *IEEE Power Energy Mag.*, vol. 9, no. 4, pp. 54–64, Jul.–Aug. 2011.

[2] A. Kwasinski, W. Weaver, P. Chapman, and P. Krein, Hurricane Katrina: Damage Assessment of Power Infrastructure for Distribution, Telecommunication, and Backup, Tech. Rep. UILU-ENG-2006-2511, CEME-TR-06-05, Aug. 2006.

[3] A. Tang, “Telecommunications performance—May 2008, Wenchuan, Sichuan earthquake,” in *Proc. TCLEE 2009: Lifeline Earthquake Engineering in a Multihazard Environment*, pp. 1407–1415.

[4] A. Kwasinski and P. T. Krein, “Telecom power planning for natural and man-made disasters,” in *Proc. INTELEC 2007*, 2007, pp. 216–222.

[5] R. Zamora and A. Srivastava, “Controls for microgrids with storage: Review, challenges, and research needs,” *Renew. Sustain. Energy Rev.*, vol. 14, pp. 2009–2018, 2010.

[6] H. Wei, H. Zijun, F. Li, T. Hongliang, and Z. Li, “Reliability evaluation of microgrid with PV-WG hybrid system,” in *Proc. Int. Conf. Electric Utility Deregulation and Restructuring and Power Technologies (DRPT)*, 2011, pp. 1629–1632.

[7] P. Costa and M. Matos, “Assessing the contribution of microgrids to the reliability of distribution networks,” *Elect. Power Syst. Res.*, vol. 79, pp. 382–389, 2009.

[8] R. H. Lasseter, “Smart distribution: Coupled microgrids,” *Proc. IEEE*, vol. 99, no. 6, pp. 1074–1082, Jun. 2011.

[9] H. Jiayi, J. Chuanwen, and X. Rong, “A review on distributed energy resources and microgrid,” *Renew. Sustain. Energy Rev.*, vol. 12, pp. 2472–2483, 2008.

[10] US DOE, The NETL Modern Grid Initiative. A Vision for The Modern Grid, Mar. 5, 2012. [Online]. Available: http://enterprise.alcatel-lucent.com/private/active_docs/NETL%20Vision%20for%20the%20Modern%20Grid.pdf.

[11] A. Kwasinski, “Technology planning for electric power supply in critical events considering a bulk grid, backup power plants, and micro-grids,” *IEEE Syst. J.*, vol. 4, no. 2, pp. 167–178, Jun. 2010.

[12] K. Hirose, T. Takeda, and S. Muroyama, “Study on field demonstration of multiple power quality levels system in sendai,” in *Proc. INTELEC*, 2006, pp. 256–261.

[13] A. Kwasinski, “Local energy storage as a decoupling mechanism for interdependent infrastructures,” in *Proc. 2011 IEEE Int. Systems Conf.*, 2011, pp. 435–441.

[14] W. Allen and S. Natale, “Achieving ultra-high system availability in a battery-less—48 V DC power plant,” in *Proc. INTELEC*, 2002, pp. 287–294.

[15] *IEEE Standard for Interconnecting Distributed Resources With Electric Power Systems*, IEEE Standards 1547-2003, 2003.

[16] C. Marnay, “Microgrids and heterogeneous security, quality, reliability, and availability,” in *Proc. Power Conversion Conf. (PCC)*, 2007, pp. 629–634.

[17] C. Nayar, M. Tang, and W. Suponthana, “Wind/PV/diesel micro grid system implemented in remote islands in the republic of maldives,” in *Proc. IEEE Int. Conf. Sustainable Energy Technologies (ICSET)*, 2008, pp. 1076–1080.

[18] J. Lopes, C. Moreira, and A. Madureira, “Defining control strategies for microgrids islanded operation,” *IEEE Trans. Power Syst.*, vol. 21, no. 2, pp. 916–924, May 2006.

[19] S. Kennedy, “Reliability evaluation of islanded microgrids with stochastic distributed generation,” in *IEEE PES’09*, 2009, pp. 1–8.

[20] R. Yokoyama, T. Niimura, and N. Saito, “Modeling and evaluation of supply reliability of microgrids including PV and wind power,” in *Proc. Power and Energy Society General Meeting*, 2008, pp. 1–5.

[21] M. Tanrioven, “Reliability and cost benefits of adding alternate power sources to an independent micro-grid community,” *J. Power Sources*, vol. 150, pp. 136–149, 2005.

[22] Z. Li, Y. Yuan, and F. Li, “Evaluating the reliability of islanded microgrid in an emergency mode,” in *Proc. 45th Int. Universities Power Engineering Conf. (UPEC)*, 2010, pp. 1–5.

[23] *IEEE Guide for Electric Power Distribution Reliability Indices*, IEEE Standards 1366-2003, 2003.

[24] A. Kwasinski, “Quantitative evaluation of DC micro-grids availability: Effects of system architecture and converter topology design choices,” *IEEE Trans. Power Electron.*, vol. 26, no. 3, pp. 835–851, Mar. 2011.

[25] Y. Luo, L. Wang, G. Zhu, and G. Wang, “Network analysis and algorithm of microgrid reliability assessment,” in *Proc. Power and Energy Engineering Conf. (APPEEC)*, 2010, pp. 1–4.

[26] C. Marnay, J. Lai, M. Stadler, and A. Siddiqui, "Added value of reliability to a microgrid: Simulations of three California buildings," in *Proc. CIGRE/IEEE PES Joint Symp. Integration of Wide-Scale Renewable Resources Into the Power Delivery System*, Jul. 2009, pp. 1–8.

[27] T. K. Panigrahi, S. Chowdhury, S. P. Chowdhury, N. Chakraborty, and Y. H. Song, "Control & reliability issue of efficient microgrid operation using hybrid distributed energy distributed energy resources," in *Proc. PSCE'06*, 2006, pp. 797–802.

[28] A. Burgio, D. Menniti, A. Pinnarelli, and N. Sorrentino, "Reliability studies of a PV-WG hybrid system in presence of multi-micro storage systems," in *Proc. IEEE PowerTech*, Bucharest, Romania, 2009, pp. 1–5.

[29] M. Datta, T. Senjyu, A. Yona, T. Funabashi, and C.-H. Kim, "A coordinated control method for leveling PV output power fluctuations of PV: Diesel hybrid systems connected to isolated power utility," *IEEE Trans. Energy Convers.*, vol. 24, no. 1, pp. 153–162, Mar. 2009.

[30] Y. Liu and C. Singh, "Nodal reliability evaluation of impact of hurricanes on transmission and distribution systems," in *Proc. Joint Int. Conf. Power Electronics, Drives and Energy Systems (PEDES) & 2010 Power India*, 2010, pp. 1–6, 20–23.

[31] I. S. Bae and J. O. Kim, "Reliability evaluation of customers in a microgrid," *IEEE Trans. Power Syst.*, vol. 23, no. 3, pp. 1416–1422, Aug. 2008.

[32] A. K. Basu, S. Chowdhury, and S. P. Chowdhury, "Impact of strategic deployment of CHP-based DERs on microgrid reliability," *IEEE Trans. Power Del.*, vol. 25, no. 3, pp. 1697–1705, Jul. 2010.

[33] P. S. Patra, J. Mitra, and S. J. Ranade, "Microgrid architecture: A reliability constrained approach," in *Proc. IEEE Power Engineering Society Meeting*, 2005, vol. 3, pp. 2372–2377.

[34] J. Mitra, S. B. Patra, and S. J. Ranade, "Reliability stipulated microgrid architecture using particle swarm optimization," in *Proc. PMAPS*, 2006, p. 7.

[35] A. K. Basu *et al.*, "Reliability study of a micro-grid power system," in *Proc. UPEC*, 2008, p. 4.

[36] J. W. Kimball, B. T. Kuhn, and R. S. Balog, "A system design approach for unattended solar energy harvesting supply," *IEEE Trans. Power Electron.*, vol. 24, no. 2, pp. 952–962, Apr. 2009.

[37] A. Villemeur, *Reliability, Availability, Maintainability, and Safety Assessment*. West Sussex, U.K.: Wiley, 1992, vol. 1, Methods and Techniques.

[38] J. S. Milton and J. C. Arnold, *Introduction to Probability and Statistics*, 3rd ed. New York: McGraw-Hill, 1995.

[39] U.S. Department of Defense, Reliability Prediction of Electronic Equipment, Feb. 1995, MIL-HDBK-217.

[40] D. Robinson *et al.*, Impact of Distributed Energy Resources on the Reliability of a Critical Telecommunications Facility, Sandia National Laboratories and National Renewable Energy Laboratory Report SAND2006-1277, Mar. 2006.

[41] S. H. Conrad, R. J. LeClaire, G. P. O'Reilly, and H. Uzunalioglu, "Critical national infrastructure reliability modeling and analysis," *Bell Labs Tech. J.*, vol. 11, no. 3, pp. 57–71, 2006.

[42] R. G. Kasilingam, *Logistics and Transportation, Design and Planning*. Dordrecht, The Netherlands: Kluwer, 1998.

[43] M. G. H. Bell and C. Cassir, *Reliability of Transport Networks*. Baldock, Hertfordshire, U.K.: Research Studies Press, 2000.

[44] J. Dong and H. S. Mahmassani, "Flow breakdown and travel time reliability," *Transportation Research Record—Traffic Flow Theory, Characteristics, and Simulations Models*, pp. 203–212, TRR 2124, 209.

[45] N. Wang, J.-C. Lu, and P. Kvam, "Reliability modeling in spatially distributed logistics systems," *IEEE Trans. Reliab.*, vol. 55, no. 3, pp. 525–534, Sep. 2006.

[46] R. Nair and E. Miller-Hooks, "Evaluation of relocation strategies for emergency medical service vehicles," *Transportation Research Record—Security, Emergencies, Management and School*, pp. 63–73, TRR 2137, 209.

[47] V. G. Kulkarni, *Modeling and Analysis of Stochastic Systems*, 2nd ed. Boca Raton, FL: CRC, 2010.

[48] R. Billington and R. N. Allan, *Reliability Evaluation of Power Systems*. New York: Plenum, 1984.

Alexis Kwasinski (S'03–M'07) received the B.S. degree in electrical engineering from the Buenos Aires Institute of Technology (ITBA), Buenos Aires, Argentina, the Graduate Specialization degree in telecommunications from the University of Buenos Aires, Buenos Aires, in 1997, and the M.S. and Ph.D. degrees in electrical engineering from the University of Illinois at Urbana-Champaign in 2005 and 2007, respectively.

From 1993 to 1997, he was with the Telefonica of Argentina for four years designing and planning telephony outside plant networks. Then, he was with Lucent Technologies Power Systems (later Tyco Electronics Power Systems) for five years as a Technical Support Engineer and a Sales Technical Consultant in Latin America. For three years, he was also a part-time instructor in charge of ITBA's Telecommunications Laboratory. He is currently an Assistant Professor in the Department of Electrical and Computer Engineering, The University of Texas at Austin. His current research interests include power electronics, distributed generation, renewable and alternative energy, smart grids, and analysis of the impact of natural disasters on critical power infrastructure, which included site damage assessments after several natural disasters in Japan, New Zealand, the U.S., and Chile.

Dr. Kwasinski was a member of the Executive Committee of the Argentine Electrotechnical Association during the years 1994 and 1995. In 2005, he was awarded the Joseph J. Suozzi INTELEC Fellowship, and in 2007, he received the best technical paper award at INTELEC. In 2009, he received the National Science Foundation (NSF) CAREER Award, and in 2011, he received an IBM Faculty Innovation Award. He is an Associate Editor for the IEEE TRANSACTIONS ON ENERGY CONVERSION.

Vaidyanathan Krishnamurthy (S'11) received the B.E. degree in electrical and electronics engineering from the Rashtreeya Vidyalaya College of Engineering (RVCE), Bangalore, India, in 2006 and the M.S. degree in electrical and computer engineering from the University of Texas at Austin in 2010. He is currently working toward the Ph.D. degree in the Electrical and Computer Engineering Department at the University of Texas at Austin.

His research interests are in dynamical systems and statistical modeling applied to power systems.

Junseok Song (S'06) received the B.S. degree in electrical and computer engineering from Hanyang University, Seoul, Korea, in 2004, and the M.S.E. degree in electrical engineering from the University of Texas at Austin in 2008, where he is currently working toward the Ph.D. degree in electrical engineering.

Ratnesh Sharma (M'10) received the B.Tech. (Hons.) degree from the Indian Institute of Technology, Kharagpur, and the M.S./Ph.D. degree from the University of Colorado at Boulder.

He leads the Energy Management Department at NEC Laboratories America, Inc., Cupertino, CA. Prior to joining NEC Labs, he was a Principal Scientist at Hewlett-Packard Labs. His research interests span sustainable energy management in electricity, buildings and transportation sectors including energy conversion, power systems, communications and analytics. He has authored more than 135 papers/technical reports and holds 60 U.S. patents.